Published in final edited form as:
J Biol Chem. 2006 January 13; 281(2): 1188–1195.

Structural Basis for Reduced Staphylocoagulase-mediated Bovine Prothrombin Activation*

Rainer Friedrich[‡,1], **Peter Panizzi**[§,1,2], **Shun-Ichiro Kawabata**[¶], **Wolfram Bode**[‡], **Paul E. Bock**[§,3], and **Pablo Fuentes-Prior**[||]

‡ *Proteinase Research Group, Max Planck Institute of Biochemistry, D-82152 Martinsried, Germany*

§ *Department of Pathology, Vanderbilt University School of Medicine, Nashville, Tennessee 37232-2561*

¶ *Department of Biology, Kyushu University, Fukuoka 812-8581, Japan*

|| *Cardiovascular Research Center, Institut Català de Ciències Cardiovasculars-Consejo Superior de Investigaciones Cientificas, Hospital de la Santa Creu i Sant Pau, 08025 Barcelona, Spain*

Abstract

Staphylocoagulase (SC) is a protein secreted by the human pathogen, *Staphylococcus aureus*, that activates human prothrombin (ProT) by inducing a conformational change. SC-bound ProT efficiently clots fibrinogen, thus bypassing the physiological blood coagulation pathway. The crystal structure of a fully active SC fragment, SC-(1–325), bound to human prethrombin 2 showed that the SC-(1–325) N terminus inserts into the Ile^{16} pocket of prethrombin 2, thereby inducing expression of a functional catalytic site in the cognate zymogen without peptide bond cleavage. As shown here, SC-(1–325) binds to bovine and human ProT with similar affinity but activates the bovine zymogen only very poorly. By contrast to the ~2-fold difference in chromogenic substrate kinetic constants between human thrombin and the SC-(1–325)·human (pro)throm-bin complexes, SC-(1–325)·bovine ProT shows a 3,500-fold lower k_{cat}/K_m compared with free bovine thrombin, because of a 47-fold increase in K_m and a 67-fold decrease in k_{cat}. The SC-(1–325)·bovine ProT complex is ~5,800-fold less active compared with its human counterpart. Comparison of human and bovine fibrinogen as substrates of human and bovine thrombin and the SC-(1–325)· (pro)thrombin complexes indicates that the species specificity of SC-(1–325) cofactor activity is determined primarily by differences in conformational activation of bound ProT. These results suggest that the catalytic site in the SC-(1–325)·bovine ProT complex is incompletely formed. The current crystal structure of SC-(1–325) ·bovine thrombin reveals that SC would dock similarly to the bovine proenzyme, whereas the bovine (pro)thrombin-characteristic residues Arg^{144} and Arg^{145} would likely interfere with insertion of the SC N terminus, thus explaining the greatly reduced activation of bovine ProT.

Pathogenic bacteria exploit and subvert several host processes and signaling pathways (1). For example, some secreted or cell wall-bound bacterial proteins can efficiently activate trypsin-like serine proteinase zymogens circulating in the blood plasma of the host. From a mechanistic point of view, these bacterial activators can be grouped into proteolytic and nonproteolytic ones (2). The former class comprises proteinases capable of cleaving host zymogens at their

*This work was supported by National Institutes of Health Grant HL071544 (to P. E. B.) and SFB 469 of the Deutsche Forschungsgemeinschaft and the Fonds der Chemischen Industrie (to W. B.).

[3] To whom correspondence should be addressed: Dept. of Pathology, Vanderbilt University School of Medicine, C3321A Medical Center North, Nashville, TN 37232-2561. Tel.: 615-343-9863; Fax: 615-322-1855; E-mail: paul.bock@vanderbilt.edu.

[1] These authors contributed equally to this work.

[2] Supported in part by National Institutes of Health Training Grant HL07751.

The atomic coordinates and structure factors (code 2A1D) have been deposited in the Protein Data Bank, Research Collaboratory for Structural Bioinformatics, Rutgers University, New Brunswick, NJ (http://www.rcsb.org/).

physiologic Arg^{15}-$(Ile/Val)^{16}$ activation sites (using the chymotrypsinogen numbering for the catalytic domain residues of serine proteinases). This cleavage liberates a new N terminus with a typical $(Ile/Val)^{16}$-$(Val/Ile)^{17}$ sequence, which inserts into the preformed "Ile^{16} pocket" of the zymogen and engages in a strong salt bridge with the Asp^{194} carboxylate. The corresponding rotation of the Asp^{194} side chain induces formation of a functional active site (for a recent review on zymogen activation mechanisms see Ref. 3). The plasminogen (Pg)[4] activator from *Yersinia pestis* (*i.e.* Pla proteinase), and related membrane-bound omptins belong to this class of bacterial activators (4,5).

The second group of activators is formed by several nonenzymatic proteins, which upon binding induce functional active sites in their cognate serine proteinase zymogens. Proteolysis of the Arg^{15}-$(Ile/Val)^{16}$ bond is not needed for activation but can occur as an epiphenomenon of the activation mechanism (6,7). Notably, these bacterial activators can modify the specificity of the bound host proteinase toward macromolecular substrates by providing novel docking sites for substrate recognition (8). The mechanism of nonproteolytic, cofactor-induced activation has been intensively investigated for streptokinase (SK), a Pg activator secreted by *β*-hemolytic streptococci (9,10), as well as for staphylocoagulase (SC), a prothrombin (ProT) activator from *Staphylococcus aureus* (11–13). Another Pg activator from *S. aureus*, staphylokinase, is structurally related to SK (8,14) but requires active plasmin (Pm) to form an activator complex of free Pg molecules (15,16).

The N-terminal sequences of SK and SC ($^{SK}Ile^{1}$-Ala-Gly and $^{SC}Ile^{1}$-Val-Thr, respectively; superscripts identify cofactor residues) mimic those of mature trypsin-like catalytic domains. These conformational zymogen activators are thought to be necessary to spread and maintain infections by their respective Gram-positive pathogens. Species-specific zymogen activation by SK and SC is a well documented and poorly understood caveat to their cofactor function. SK is highly specific for conformational activation of human Pg among other species, but the catalytic SK·Pg/Pm complexes proteolytically activate Pg from a broad range of species (17). The resistance of murine Pg to activation by SK has impeded the development of versatile animal models of human streptococcal infection. As elegantly shown recently in a transgenic mouse model expressing only human Pg, tissue invasion by the human pathogen *Streptococcus pyogenes* is critically dependent on human Pg, SK, and the bacterial Pg/Pm-binding M-like protein (*i.e.* PAM) to generate Pm that degrades fibrin and the extracellular matrix (18). Given the conservation in sequence and fold exhibited by members of the chymotrypsinogen family of serine proteinases across species, the high specificity of SC for activation of human ProT is similarly quite remarkable. Here we present for the first time peptide substrate and Fbg clotting studies that establish limits on the ability of SC-(1–325) to activate bovine ProT compared with human ProT and the effect of SC-(1–325) binding on bovine thrombin activity. The results suggest that compared with SC-(1–325)·human ProT, the catalytic site in SC-(1–325)·bovine ProT is incompletely formed. Surprisingly, equilibrium binding results indicate that SC-(1–325) binds bovine ProT with a 1 to 1 stoichiometry and only ~12-fold weaker than to the human zymogen. We also present the crystal structure of SC-(1–325) bound to bovine *α*-thrombin, along with a more detailed description and comparison of the atomic interactions in the SC-(1–325)·human (pre)thrombin and SC-(1–325)·bovine thrombin complexes to define structural differences responsible for the species specificity of ProT activation by SC.

[4]The abbreviations used are: Pg, plasminogen; SC, staphylocoagulase; SC-(1–325), staphylocoagulase fragment, residues 1–325; D1, crystallographically defined domain 1 of SC, residues 1–142; D2, crystallographically defined domain 2 of SC, residues 150 –281; Fbg, fibrinogen; [OG]FPR-ProT, N^{α}-[(acetylthio)acetyl]-D- Phe-Pro-Arg-chloromethyl ketone-inactivated ProT labeled with 5-(and 6)-iodoacetamido-2′,7′-difluorofluorescein; *p*NA, *p*-nitroaniline; ProT, prothrombin; Pm, plasmin; SK, streptokinase; Pre 2, prethrombin 2, the product of cleavage of ProT at Arg^{271}-Thr^{272}.

EXPERIMENTAL PROCEDURES

Protein Purification and Characterization

SC Ile^{1}-Gln^{325} (SC-(1–325)) from *S. aureus* Newman, Tager strain 104, or strain BB were expressed and purified according to published procedures (12) or purified by diethyl aminoethyl chromatography, respectively. SC-(1–325) was shown previously to activate human ProT and to form an SC-(1–325)·ProT complex with similar Fbg clotting activity to α-thrombin (12,19). Human ProT was labeled specifically at the catalytic site with 5-(and 6)-(iodoacetamido)-2′,7′-difluorofluorescein (Oregon Green 488 iodoacetamide) ([OG]FPR-ProT) as described previously (20). Bovine ProT and α-thrombin (Hematologic Technologies Inc.) were dialyzed into 50 mM Hepes, 110 mM NaCl, 5 mM $CaCl_2$, 1 mg/ml polyethylene glycol 8000, pH 7.4, quick-frozen, and stored at −80 °C. Protein concentrations were determined by absorbance at 280 nm with the following absorption coefficients $((mg/ml)^{-1}\ cm^{-1})$ and molecular weights: human ProT, 1.47, 71,600; human thrombin, 1.74, 36,600; human Fbg, 1.54, 340,000; bovine Fbg, 1.51, 330,000; SC-(1–325), 1.00, 38,000; bovine ProT, 1.44, 72,100; and bovine thrombin, 1.95, 36,700 (20–22).

Chromogenic Substrate Kinetics and Fbg Clotting Activity

Hydrolysis of the thrombin substrate, H-D-Phe-Pip-Arg-*p*NA by bovine α-thrombin and the SC-(1–325)·bovine (pro)thrombin complexes was followed by monitoring the absorbance increase at 405 nm in 50 mM Hepes, 110 mM NaCl, 5 mM $CaCl_2$, 1 mg/ml polyethylene glycol 8000, pH 7.4 buffer containing 1 mg/ml bovine serum albumin and 0.1 mg/ml soybean trypsin inhibitor, at 25 °C. Stoichiometric factors (n) were determined by fitting of the quadratic binding equation to initial rates of hydrolysis of 100 μM H-D-Phe-Pip-Arg-*p*NA by bovine α-thrombin (1 nM) or bovine ProT (50 nM) as a function of the total SC-(1–325) concentration. The kinetic parameters, k_{cat}, K_m, and K_i for the product, when appropriate, were determined by simultaneous fits of the integrated Michaelis-Menten equation including competitive product inhibition to full reaction progress curves determined at H-D-Phe-Pip-Arg-*p*NA concentrations of 15, 31, and 62 μM with 1 nM bovine thrombin in presence or absence of saturating SC-(1–325). For SC-(1–325)·bovine ProT cleavage of H-D-Phe-Pip-Arg-*p*NA, kinetic parameters were determined by fitting the Michaelis-Menten equation to initial rates collected over a substrate concentration range of 0–4 mM. In all of the assays, SC-(1–325) and bovine (pro)thrombin were preincubated for at least 20 min, and the reactions were initiated by the addition of substrate. Fbg clotting activity relative to a human thrombin standard was measured with a fibrometer from the slopes of plots of clotting time against the reciprocal of the enzyme concentration essentially as described (19,23).

Competitive Binding of SC-(1–325) to Native Bovine ProT and Human [OG]FPR-ProT Measured by Fluorescence

The effect of native bovine ProT on SC-(1–325) binding to 0.11 nM [OG]FPR-ProT was measured in fluorescence titrations with native bovine ProT, at fixed concentrations of SC-(1–325) (1, 11, and 110 nM), following a previously detailed procedure (20). Direct titration of [OG]FPR-ProT with SC-(1–325) in the picomolar range was performed by incubation of individual reactions for ≥16 h in the dark to assure that equilibrium had been reached. These long incubations were not necessary for titrations at probe concentrations in the nanomolar range. Fluorescence measurements of individual binding reactions and analysis of competitive binding were performed as described in the companion paper (20). The error estimates represent ± 2 S.D.

Crystallization and Structure Solution

Bovine ProT was purified from fresh ox blood and activated using *Oxyuranus scutellatus* venom (Latoxan). Thrombin was inhibited with D-Phe-Pro-Arg-chloromethyl ketone (Bachem) and mixed with an equimolar amount of purified SC-(1–325). The complex was purified by anion exchange chromatography on a TSK gel DEAE-5PW column (Tosoh Bioscience) and concentrated using Centricon YM 30 filters (Millipore). Crystals grew out of solutions containing 0.1 M imidazole, pH 7.0–7.5, 0.2 M ammonium formate, 12% polyethylene glycol 4,000. These crystals diffracted only to medium resolution but allowed collection of a complete data set "in house" from a single crystal mounted on a capillary, using a MAR345 image plate system (Marresearch) installed on a RIGAKU rotating anode generator (Rigaku Corp.). The data were processed with MOSFLM (www.mrc-lmb.cam.ac.uk/harry/mosflm/) and scaled and reduced using programs supported by CCP4 (www.ccp4.ac.uk/main.html). The structure was solved by molecular replacement using the coordinates of the corresponding human complex as search model and refined using data to 3.5 Å resolution with programs of the CNS suite (xplor.csb.yale.edu/cns_solve/). Strong noncrystallographic restraints were applied throughout refinement. The atomic coordinates of the SC-(1–325)·bovine α-thrombin complex have been deposited in the Protein Data Bank under accession code 2A1D.

RESULTS

Activation of Bovine ProT by SC-(1–325) and Its Effect on Bovine α-Thrombin Activity

There have been conflicting reports regarding the species specificity of SCs from different isolates. SC from strain Tager 104 was reported to protect human thrombin, but not bovine thrombin, from antithrombin-mediated inhibition (24). More recently, Raus and Love (25) reported qualitative differences in the clotting activities of SCs isolated from *Staphylococcus intermedius* and *S. aureus* from different animal sources when their complexes with human or bovine ProT were probed against human, bovine, or equine Fbg. No affinity constants have been determined for ProT from various species, however, so it remains to be clarified whether these differences result from impaired ProT activation because of loss of affinity or loss of activity or because the SC·ProT activator complex is unable to cleave substrate Fbg.

We compared the cofactor activities of SC-(1–325) against human ProT and its bovine homolog. Despite the high similarities both at the sequence and structural level of human and bovine thrombin (81% overall and 87% catalytic domain sequence identity, respectively; ~0.45 Å root mean square deviation of all defined α-carbon atoms in the catalytic domains (26)), SC-(1–325) was a much poorer activator of bovine ProT. The reason for this puzzling observation is clarified below.

Chromogenic substrate kinetic studies were performed to determine the effects of SC-(1–325) on activation of bovine ProT and on the activity of bovine thrombin. SC-(1–325) activated bovine ProT with a stoichiometric factor of 0.85 ± 0.07 mol SC-(1–325)/mol ProT and with a maximal rate of 0.051 ± 0.003 ΔA_{405} nm/min at 50 nM SC-(1–325)·bovine ProT complex and 100 μM H-D-Phe-Pip-Arg-*p*NA (Fig. 1). SC-(1–325) binding to bovine α-thrombin resulted in a 1.9-fold hyperbolic decrease in the rate of substrate hydrolysis by the complex, characterized by a stoichiometry of 1.1 ± 0.6 mol SC-(1–325)/mol thrombin and an apparent dissociation constant (K_D) of 0.3 ± 0.2 nM (Fig. 1). The results demonstrated that SC-(1–325) bound both bovine ProT and α-thrombin and that the SC-(1–325)·bovine ProT complex was ~60-fold less active as compared with the SC-(1–325)·human ProT complex under the conditions of the assays, indicating that SC-(1–325) is a much more effective activator of the human zymogen.

The effect of SC-(1–325) on the chromogenic substrate activity of bovine thrombin was examined further by full progress curve analysis to determine Michaelis-Menten kinetic parameters for α-thrombin and the SC-(1–325)·α-thrombin complex. In the presence of SC-(1–325), the specificity constant (k_{cat}/K_m) for bovine α-thrombin decreased 5-fold, because of a 1.4-fold decrease in k_{cat} and a 3-fold increase in K_m (Table 1). Kinetic constants determined for the SC-(1–325)·bovine ProT complex by initial rates indicated a 3,500-fold lower k_{cat}/K_m compared with free α-thrombin. In addition to the 47-fold increase in K_m, indicating significantly weaker substrate binding, k_{cat} for hydrolysis of H-D-Phe-Pip-Arg-*p*NA by the SC-(1–325)·bovine ProT complex was 1.4 ± 0.1 s^{-1} (Table 1), reduced 67-fold compared with α-thrombin. The results demonstrated that SC-(1–325) activates bovine ProT but that the activity of the complex (k_{cat}/K_m) toward H-D-Phe-Pip-Arg-*p*NA compared with the SC-(1–325)·bovine thrombin complex is 740-fold lower, whereas the SC-(1–325) complex with human ProT is ~2-fold more active than SC-(1–325)·human thrombin measured with the same substrate (20).

Fibrinogen Clotting Activities of Human and Bovine Thrombin and SC-(1–325)·(Pro)thrombin Complexes

Fbg clotting assays were performed to assess the role of the low catalytic activity of the SC-(1–325)·bovine ProT complex in bovine and human Fbg substrate recognition (Table 2). Compared with human thrombin, the SC-(1–325) complexes with human (pro)thrombin had indistinguishable activity toward human Fbg and also exhibited a similar, 3–4-fold lower activity with bovine Fbg. Bovine thrombin and SC-(1–325)·bovine thrombin complex had essentially the same activities of 67 and 96%, respectively, as human thrombin toward human Fbg and lower activities of ~30% toward bovine Fbg. By contrast, the SC-(1–325)·bovine ProT complex exhibited only 0.07% of the clotting activity of human thrombin toward human Fbg. Moreover, the clotting activity of the bovine complex with bovine Fbg was undetectable at concentrations up to 46 μM. These results indicated a small 3–4-fold dependence of the clotting activity on the species of Fbg for human and bovine thrombin and the corresponding SC-(1–325)·thrombin complexes. In these results, the 5-fold lower k_{cat}/K_m of the SC-(1–325)·bovine thrombin complex for chromogenic substrate compared with bovine thrombin (Table 1) was not reflected in the clotting activity (Table 2). Remarkably, however, the 3,470-fold lower k_{cat}/K_m for chromogenic substrate hydrolysis by the SC-(1–325)·bovine ProT complex was correlated with a 1,400-fold lower clotting activity toward human Fbg and an undetectably lower activity toward bovine Fbg. These results indicated that the greatly reduced Fbg clotting activity of the SC-(1–325)·bovine ProT complex results from its low catalytic activity and suggested a minor role for species-specific recognition of substrate Fbg.

Competitive Binding of SC-(1–325) to Native Bovine ProT and [OG]FPR-ProT

Competitive binding experiments were carried out to determine the affinity of SC-(1–325) for bovine ProT by the use of human [OG]FPR-ProT as a competitive binding probe. Simultaneous fits of direct and competitive titrations determined that SC-(1–325) bound human [OG]FPR-ProT with a stoichiometry of 1.0 ± 0.1 mol SC-(1–325)/mol labeled ProT and a dissociation constant (K_D) of 16 ± 9 pM, consistent with values determined in the companion paper (20). Analysis of competitive binding of [OG]FPR-ProT and native bovine ProT demonstrated that SC-(1–325) bound native bovine ProT with a K_D of 0.2 ± 0.1 nM (Fig. 2). These results indicated that SC-(1–325) binds very tightly to bovine ProT and suggested that high affinity binding may not be the sole determinant of effective zymogen activation by SC-(1–325).

The Two Helical Domains of SC-(1–325) Form a Continuous Structure

We have previously presented crystal structures of SC-(1–325) bound to human α-thrombin and to its immediate precursor, Pre 2 (12). We have now solved the structure of the SC-(1–

325) complex with bovine thrombin to low but still satisfactory resolution. A summary of crystallographic parameters and refinement statistics for this crystal structure is given in Table 3. All of the stereochemical parameters were better than average in structures solved at this resolution, as assessed with PROCHECK (www.biochem.ucl.ac.uk/~roman/procheck/pro-check.html). Here we present a detailed analysis of the three crystal structures, as a basis for understanding the species specificity of SC and the mechanism of Fbg processing by SC·(pro)thrombin complexes.

Each boomerang-shaped SC-(1–325) molecule consists of two α-helical domains, which stick together at an angle of about 110°. The N-terminal domain D1 (residues ^{SC}Ile^{1} to ^{SC}Gln^{142}) essentially comprises three α-helices (α_1^{D1} to α_3^{D1}), which range in length from 25 to 41 residues (Fig. 3). The three α-helices are slightly wound around each other to form a left-handed α-helical coiled-coil. The C-terminal SC domain D2 comprises residues ^{SC}Thr^{150} to ^{SC}Gly^{281} and also contains a three-helix bundle formed by helices α_1^{D2} to α_3^{D2}. The two major helix bundles are topologically similar (Fig. 4*A*) but are only distantly related at the sequence level, pointing to an early gene duplication event. The centers of the helix bundles are occupied by a number of medium-sized hydrophobic side chains, which are mainly leucine residues in D1 but more varied in D2. These side chains pack together in a “knobs-in-holes” manner, creating a quite hydrophobic core free of buried water molecules or polar groups. In addition, D2 is C-terminally extended by three shorter α-helices. Together, 75% of all defined residues of SC-(1–325) are found in segments with helical conformation in agreement with results obtained by circular dichroism (not shown).

D1 and D2 contact each other along an interface centered on the side chain of the strictly conserved linker residue ^{SC}Leu^{146}, burying a surface area of about 1,150 Å^2 from bulk solvent (Fig. 4*B*). The ^{SC}Leu^{146} side chain is enwrapped by the aliphatic parts of polar/charged residues donated by the C-terminal ends of helices α_1^{D1} and α_3^{D1} (*e.g.* the strictly conserved ^{SC}Tyr^{55}) and the N-terminal parts of α_1^{D2} and α_3^{D2}. Several of these side chains engage in a network of hydrogen bonds and salt bridges, most notably the superficial interdomain salt bridge, ^{SC}Glu^{54} … ^{SC}Arg^{209}. Together, this interface is well packed and rigid, so that the two SC domains would presumably maintain their relative orientation in solution also in the free cofactor.

The C Terminus of SC-(1–325) Is Intrinsically Disordered

The C-terminal SC-(1–325) segments from ^{SC}Glu^{282} to ^{SC}Leu^{325} are not defined by appropriate electron density in any of the six equivalent SC-(1–325) moieties of the human (pre)thrombin and bovine thrombin complexes, suggesting enhanced flexibility. Three-state secondary structure prediction methods (cubic.bioc.columbia.edu/predictprotein/), which correctly identify all major α-helices within the defined SC-(1–325) fragment, indicate with high probability that this molecular region is almost entirely solvent-exposed and devoid of regular secondary structure. An inherent disorder of this C-terminal peptide is also in agreement with VL-XT predictor analyses (www.pondr.com/), according to which most of the SC region following ^{SC}Gln^{300} is intrinsically disordered. Around the defined C termini of both SC-(1–325) molecules, the crystals contain large solvent-filled cavities, which would seem to accommodate this disordered ^{SC}Glu^{282}-^{SC}Leu^{325} segment without steric hindrance.

The D1-Thrombin Interface Differs in the Bovine and Human Thrombin Complexes

Upon SC-(1–325)·thrombin complex formation, ~3,400 Å^2 of accessible surface is removed from contact with the bulk solvent (Fig. 3). Domain 1 contacts the cognate thrombin molecule primarily at the 148 loop that borders the “south” rim of the thrombin active site (with respect to the standard orientation) (27). Of note, this loop moves considerably compared with its position in human FPR-thrombin (27), Gly^{149D} being displaced to a maximum of about 11.5

Å (Fig. 5). SC-(1–325) helicesα_1^{D1} and α_2^{D1} as well as the α_2^{D1}- α_3^{D1} connector engage in particularly extensive contacts with the indole moiety of Trp^{148}. In addition to these hydrophobic interactions, a few polar/charged contacts are observed at this SC-(1–325) ·thrombin interface. For example, the thrombin-internal Glu^{146} … Arg^{221} salt bridge becomes embedded in a hydrophobic pocket formed by the strictly or well conserved residues $^{SC}Leu^{74}$, $^{SC}Lys^{78}$, and $^{SC}Phe^{105}$, with the Arg^{221} guanidyl group frontally opposing the $^{SC}Asp^{106}$ carboxylate.

Notably, human and bovine thrombin diverge considerably in the 148 loop sequence, with mostly nonconservative substitutions Leu^{144} → Arg, Lys^{145} → Arg, Ala^{149A} → Thr, Asn^{149B} → Ser, Gly^{149D} → Ala, Glu^{149E} → Lys, and Gly^{150} → Val. These variations in turn provoke changes at the SC-thrombin interface. For example, the 149–150 segments adopt different conformations in the two thrombin complexes, but in neither case seem to make particularly specific interactions with the SC moiety (Fig. 5).

The exchanges of Leu^{144} and in particular of Lys^{145} by Arg residues in the bovine species have more dramatic consequences. In SC·human (pre)thrombin, the distal ammonium group of Lys^{145}, framed by $^{SC}Leu^{67}$, $^{SC}Gln^{71}$, and the Glu^{146}-Thr^{147} main chain segment, is fixed through favorable hydrogen bonds with $^{SC}Gln^{71}$ Oε 1, $^{SC}Asp^{70}$ Oδ1, and Glu^{146} O. By contrast, steric clashes of the bulkier Arg^{145} side chain of bovine (pro)thrombin would prohibit it to be similarly buried at the interface with SC. Indeed, Arg^{145} extends away from the thrombin moiety in the SC·bovine thrombin complex (shown in *yellow* in Fig. 6).

To insert into the Ile^{16} pocket (marked by the Asp^{194} carboxylate group at its bottom; Fig. 6) and to induce functional active and substrate binding sites, the N-terminal SC segment would have to circumvent or displace the neighboring, charged side chains of the bovine-specific (pro)thrombin residues Arg^{144} and Arg^{145}. The N-terminal $^{SC}Ile^{1}$-$^{SC}Tyr^{6}$ hexapeptide, which is flexibly disordered in both human and bovine thrombin complexes with SC-(1–325), is highlighted *green* in Fig. 6. Given the limited flexibility at the SC-(pre)thrombin interface, the exposed side chains of Arg^{144} and Arg^{145} would clash with the approaching N-terminal segment of the bound cofactor. In addition, they are likely to repel the incoming free N terminus of $^{SC}Ile^{1}$ electrostatically. As a consequence, the positively charged "gate" to the Ile^{16} pocket formed by these basic residues would efficiently hamper or even impair the correct insertion of the N terminus into the activation pocket. Thus, the energetically unfavorable approach and insertion of the N-terminal SC residues may explain the impaired activator activity of the bacterial cofactor against bovine ProT.

Comparison of Exosite I Interactions in the SC-(1–325)·Bovine and Human Thrombin Complexes

The positively charged anion-binding exosite I is extremely similar in both human and bovine (pre)thrombin. It is a slightly notched surface depression "east" of the thrombin active site centered on the 70–80 loop and bordered by the 37 loop (Fig. 3) (28,29). Its central Arg^{73}, Arg^{67}, Arg^{75}, and Arg^{77A} side chains are surrounded by other positively charged residues such as Arg^{35}, Lys^{36}, Lys^{81}, Lys^{109}, and Lys^{110}, only interspersed by a few hydrophobic side chains such as the phenolic group of Tyr^{76}. The vast majority of residues that form exosite I are strictly conserved in human and bovine thrombin. The edge residue Asn^{78} (in the human enzyme) represents an exception to this pattern of conservation, because it is replaced by a lysine in bovine thrombin. This side chain, however, is not involved in direct contacts with SC. Consequently, SC interactions with exosite I are virtually identical in the human and bovine (pro)thrombin complexes, in agreement with the similar SC affinities for both thrombin species (see above).

DISCUSSION

Although SC-(1–325) activates bovine ProT, the SC-(1–325)·bovine ProT complex is about 5,800-fold less active than its human counterpart, consistent with early reports that *S. aureus* isolates activated human ProT better than bovine ProT (25). Our studies demonstrated a low intrinsic activity of the SC-(1–325)·bovine ProT complex toward a tripeptide-*p*NA substrate, which may explain early reports of no activation of bovine ProT by SC (30).

The role of substrate Fbg and (pro)thrombin species specificity in the clotting activities of the SC-(1–325)·(pro)thrombin complexes was evaluated by comparing the activities of human and bovine thrombin and the corresponding SC-(1–325)·(pro)thrombin complexes toward both human and bovine Fbg. The results demonstrate a relatively small, 3–4-fold preference of both human and bovine thrombin as well as SC-(1–325)·thrombin complexes for human Fbg. Although cofactor complexes with human thrombin and its precursor have similar activity, the bovine SC-(1–325)·ProT complex shows a drastically reduced activity toward both human and bovine Fbg. The results support the conclusion that the low catalytic activity of SC-(1–325)·bovine ProT is mainly responsible for its low Fbg clotting activity. The species specificity of SC-(1–325) cofactor activity in ProT activation and Fbg clotting is evidently primarily due to species-specific differences in conformational activation of ProT in the SC-(1–325)·ProT complexes.

In view of these results, the similar affinity of SC-(1–325) for bovine and human ProT was unanticipated. Indeed, analysis of the competitive binding results indicated an approximate 12-fold higher affinity of SC-(1–325) for human [OG]FPR-ProT compared with bovine ProT, but this was indistinguishable from SC-(1–325) binding to native human ProT (K_D 72 ± 36 pM) (20). Because of the significant experimental error involved in determining affinities of very tight interactions, such small differences may not be meaningful. The results of our previous studies of human ProT activation with N-terminal and domain mutants of SC-(1–325) indicated that binding affinity was correlated with activation of the human ProT zymogen (12). In the case of bovine ProT, however, the low activity of the SC-(1–325)·bovine ProT complex was not associated with a significantly lower affinity of the activator for the zymogen, indicating that tight binding alone is not enough for full activation. The results suggest at least one of the following: (*a*) N-terminal insertion is much less favorable in the SC-(1–325) complex with bovine ProT as compared with the human zymogen, such that the former is only partially activated; (*b*) the SC N terminus inserts into the Ile^{16} pocket of bovine ProT but adopts a nonoptimal orientation for full ProT activation; or (*c*) zymogen activation by SC can occur at a low level independently of N-terminal insertion.

The structure of the SC-(1–325)·bovine thrombin complex supports the idea that SC N-terminal insertion is hindered in the cofactor complex with bovine ProT, mainly because of the presence of two bovine (pro)thrombin-specific residues in the 148 loop, Arg^{144} and Arg^{145}. These bulky and positively charged residues appear to repel or partially deflect the N-terminal segment of SC-(1–325), thus favoring either conformations of the complex with an exposed cofactor N terminus and/or a less than optimal positioning of the $^{SC}Ile^{1}$ α-amino group in the ProT Ile^{16} pocket. Lastly, we confirmed our previous observation that a variant lacking the N-terminal $^{SC}Ile^{1}$-$^{SC}Val^{2}$ dipeptide, SC-(3–325), retains ~2% activator activity of SC-(1–325) toward human ProT (results not shown), indicating that a low level of conformational activation without N-terminal insertion cannot be ruled out completely.

Our crystal structures of SC-(1–325) bound to human and bovine thrombin, together with that of the SC-(1–325)·human Pre 2 complex, allow for a dissection of molecular events during ProT binding and activation. First, we notice that in these three complexes the interactions of SC-(1–325) domains D2 and D1 with exosite I and the 148 loop, respectively, are almost

identical. Exosite I is in a precursor, low affinity state in ProT (proexosite I) (31), whereas the more solvent-exposed, longer 148 loop is commonly disordered in thrombin crystal structures. Therefore, considering the excellent electrostatic complementarity of the two surfaces, it appears reasonable to assume that docking of the more C-terminal D2 to proexosite I represents the initial binding event. This strong electrostatic interaction stabilizes proexosite I in its active, thrombin-like conformation. Further, because D1 and D2 are rigidly connected, the N-terminal domain D1 would be appropriately positioned to dock the tip of the 148 loop into a shallow hydrophobic groove. The entropic penalty of stabilizing this long flexible loop is compensated for by a multitude of van der Waals' and electrostatic interactions, most notably with the indole moiety of the thrombin-specific Trp^{148}.

Finally, positioning of D1 locates the N-terminal activation hexapep-tide $^{SC}Ile^{1}$-$^{SC}Tyr^{6}$ at the correct distance to insert into the Ile^{16} pocket of the zymogen, triggering the Asp^{194} side chain rotation linked to functional active site generation in a manner similar to the endogenous Ile^{16} N terminus formed upon proteolytic activation. The latter step is essential for cofactor-induced activation, because deletion of the $^{SC}Ile^{1}$-$^{SC}Val^{2}$ dipeptide reduces SC activator activity ~98% (12).

We reported previously that both Met-SC-(1–325) and the truncated form, SC-(2–325) generate complexes of only slightly different maximal activity with human ProT, whereas their affinities for the zymogen are 60- and 6-fold lower than SC-(1–325), respectively (12). These unanticipated findings imply that presentation of a free N terminus that can reach into the Ile^{16} pocket is more critical for activation than both the exact nature of the N-terminal residue and the conformation of the preceding segment. The substantially higher affinity for activation of ProT by the truncated variant is explained by the close physicochemical similarity of its N-terminal $^{SC}Val^{2}$ to the natural $^{SC}Ile^{1}$ residue, as compared with the nonbranched $^{SC}Met^{0}$ of Met-SC-(1–325) and its ability to extend into the activation pocket.

Contrasting with these observations, SK-mediated Pg activation more strictly requires the N-terminal $^{SK}Ile^{1}$ residue (32). The crystal structure of SK bound to the Pm catalytic domain reveals that the first residue defined by electron density, $^{SK}Ser^{12}$, is located ~21 Å away from the endogenous Ile^{16} residue (10). Considering that the similarity of catalytic domains of thrombin and Pm implies conserved interactions of the N-terminal cofactor residue with the Ile^{16} pocket, we predict that the N-terminal SK segment approaches Pg in a more extended conformation compared with the SC-(1–325)·Pre 2 complex and that the impaired activator activity of the $^{SK}Ile^{1}$-deleted variant results from the inability of $^{SK}Ala^{2}$ to reach the zymogen Ile^{16} pocket.

A previously unappreciated effect of fixing the (pro)thrombin 148 loop conformation by cofactor binding is the deflection of residues that might interfere with insertion of the activation peptide into the Ile^{16} pocket. Unexpectedly, bovine thrombin, although engaging in similar overall interactions with SC-(1–325), differs from its human counterpart in the location of several side chains of the 148 loop, most notably the pair of consecutive basic residues, Arg^{144} and Arg^{145}. These bulky side chains would seem to interfere directly with an incoming $^{SC}Ile^{1}$-$^{SC}Tyr^{6}$ segment, both through direct steric hindrance and by generating a positively charged region that repels the N terminus of SC. This finding adds a new example to the reported phenomenon of coevolution of host and bacterial proteins, as recently reported for the SK-Pg system (33).

References

1. Finlay BB, Falkow S. Microbiol Mol Biol Rev 1997;61:136–169. [PubMed: 9184008]
2. Boyle MD, Lottenberg R. Thromb Haemostasis 1997;77:1–10. [PubMed: 9031440]

3. Khan A, James M. Protein Sci 1998;7:815–836. [PubMed: 9568890]
4. Sodeinde OA, Subrahmanyam YV, Stark K, Quan T, Bao Y, Goguen JD. Science 1992;258:1004–1007. [PubMed: 1439793]
5. Vandeputte-Rutten L, Kramer RA, Kroon J, Dekker N, Egmond MR, Gros P. EMBO J 2001;20:5033–5039. [PubMed: 11566868]
6. Boxrud PD, Bock PE. J Biol Chem 2004;279:36642–36649. [PubMed: 15215239]
7. Boxrud PD, Verhamme IM, Bock PE. J Biol Chem 2004;279:36633–36641. [PubMed: 15215240]
8. Parry MA, Fernandez-Catalan C, Bergner A, Huber R, Hopfner KP, Schlott B, Guhrs KH, Bode W. Nat Struct Biol 1998;5:917–923. [PubMed: 9783753]
9. Castellino FJ, Sodetz JM, Brockway WJ, Siefring GE Jr. Methods Enzymol 1976;45:244–257. [PubMed: 1011996]
10. Wang X, Lin X, Loy JA, Tang J, Zhang XC. Science 1998;281:1662–1665. [PubMed: 9733510]
11. Hemker HC, Bas BM, Muller AD. Biochim Biophys Acta 1975;379:180–188. [PubMed: 1115793]
12. Friedrich R, Panizzi P, Fuentes-Prior P, Richter K, Verhamme I, Anderson PJ, Kawabata S, Huber R, Bode W, Bock PE. Nature 2003;425:535–539. [PubMed: 14523451]
13. Kawabata S, Morita T, Iwanaga S, Igarashi H. J Biochem (Tokyo) 1985;98:1603–1614. [PubMed: 4093448]
14. Rabijns A, De Bondt HL, De Ranter C. Nat Struct Biol 1997;4:357–360. [PubMed: 9145104]
15. Collen D, Schlott B, Engelborghs Y, Van Hoef B, Hartmann M, Lijnen HR, Behnke D. J Biol Chem 1993;268:8284–8289. [PubMed: 8463338]
16. Grella DK, Castellino FJ. Blood 1997;89:1585–1589. [PubMed: 9057640]
17. McCoy HE, Broder CC, Lottenberg R. J Infect Dis 1991;164:515–521. [PubMed: 1869838]
18. Sun H, Ringdahl U, Homeister JW, Fay WP, Engleberg NC, Yang AY, Rozek LS, Wang X, Sjobring U, Ginsburg D. Science 2004;305:1283–1286. [PubMed: 15333838]
19. Panizzi P, Friedrich R, Fuentes-Prior P, Richter K, Bock PE, Bode W. J Biol Chem 2006;281:1179–1187. [PubMed: 16230339]
20. Panizzi P, Friedrich R, Fuentes-Prior P, Kroh HK, Briggs J, Tans G, Bode W, Bock PE. J Biol Chem 2006;281:1169–1178. [PubMed: 16230340]
21. Mann KG, Elion J, Butkowski RJ, Downing M, Nesheim ME. Methods Enzymol 1981;80:286–302. [PubMed: 7043193]
22. Fenton JW II, Fasco MJ, Stackrow AB. J Biol Chem 1977;252:3587–3598. [PubMed: 16908]
23. Fenton JW II, Fasco MJ. Thromb Res 1974;4:809–817. [PubMed: 4858454]
24. Hendrix H, Lindhout T, Mertens K, Engels W, Hemker HC. J Biol Chem 1983;258:3637–3644. [PubMed: 6833222]
25. Raus J, Love DN. J Clin Microbiol 1991;29:570–572. [PubMed: 2037675]
26. Brandstetter H, Turk D, Hoeffken HW, Grosse D, Sturzebecher J, Martin PD, Edwards BF, Bode W. J Mol Biol 1992;226:1085–1099. [PubMed: 1518046]
27. Bode W, Mayr I, Baumann U, Huber R, Stone SR, Hofsteenge J. EMBO J 1989;8:3467–3475. [PubMed: 2583108]
28. Bode W, Turk D, Karshikov A. Protein Sci 1992;1:426–471. [PubMed: 1304349]
29. Bode, W.; Huber, R.; Rydel, T.; Tulinsky, A. Thrombin Structure and Function. Berliner, LJ., editor. Plenum Press; New York: 1992.
30. Zajdel M, Wegrzynowicz Z, Jeljaszewicz J, Pulverer G. Contrib Microbiol Immunol 1973;1:364–375. [PubMed: 4805312]
31. Anderson PJ, Nesset A, Dharmawardana KR, Bock PE. J Biol Chem 2000;275:16428–16434. [PubMed: 10748007]
32. Wang S, Reed GL, Hedstrom L. Biochemistry 1999;38:5232–5240. [PubMed: 10213631]
33. Gladysheva IP, Turner RB, Sazonova IY, Liu L, Reed GL. Proc Natl Acad Sci U S A 2003;100:9168–9172. [PubMed: 12878727]

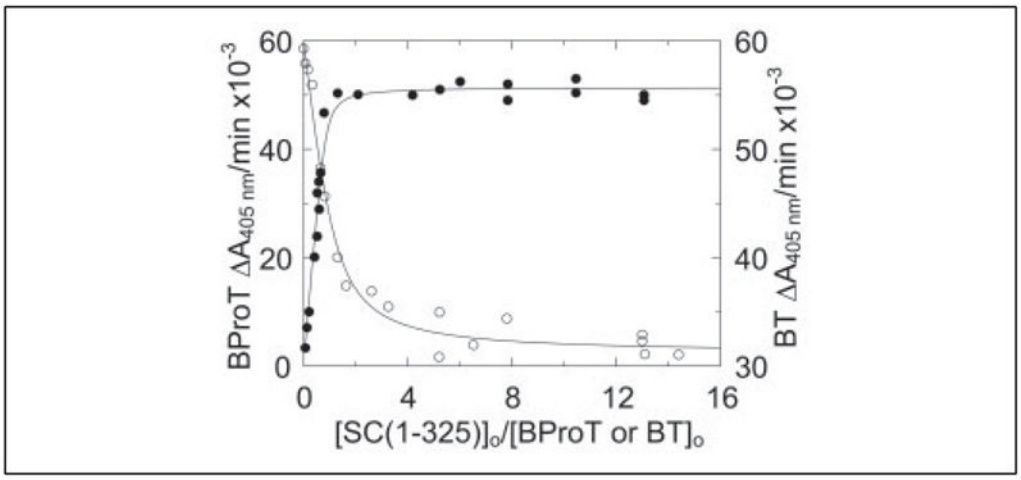

FIGURE 1. Effect of SC-(1–325) binding on activation of bovine ProT and the activity of bovineα-thrombin

Initial velocities ($\Delta A_{405\ nm}/min$) for hydrolysis of 100 μM H-D-Phe-Pip-Arg-*p*NA by 50 nM bovine ProT (*BProT*, ●) and 1 nM bovine α-thrombin (*BT*, ○) plotted as a function of the ratio of total concentrations of SC-(1–325) to BProT or BT ($[SC\text{-}(1–325)]_o/[BProT\ or\ BT]_o$). The assays were performed, and the results were analyzed as described under “Experimental Procedures.”

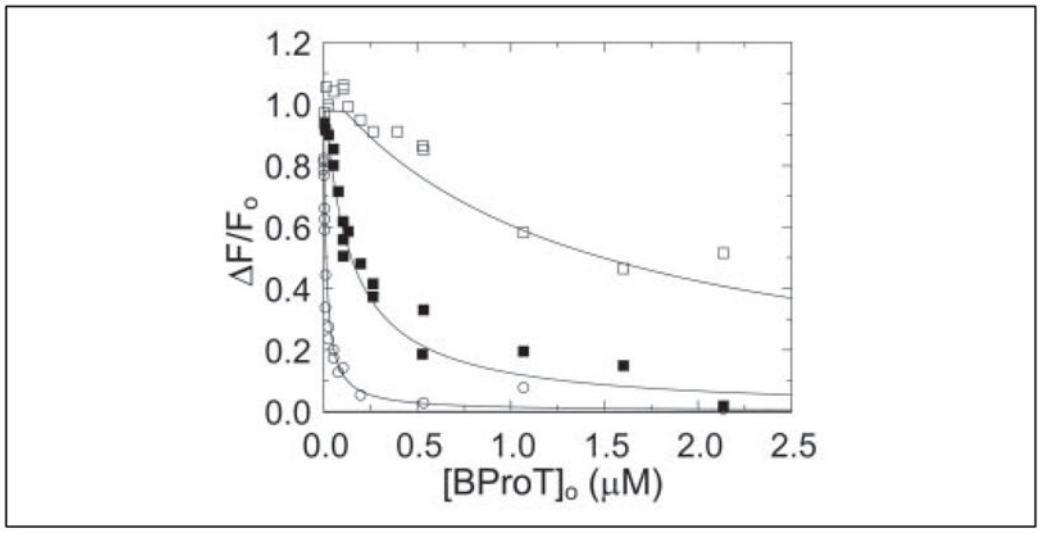

FIGURE 2. Competitive binding of SC-(1–325) to native bovine ProT and human [OG]FPR-ProT

The fractional change in fluorescence ($\Delta F/F_o$) of 0.11 nM [OG]FPR-ProT plotted against the total concentration of bovine ProT ($[BProT]_o$) at 1.1 nM (○), 11 nM (■), and 110 nM (□) SC-(1–325). The *lines* represent the fit by the cubic equation with the parameters given in the text and *n* fixed at 1. Fluorescence titrations were performed and analyzed as described under "Experimental Procedures."

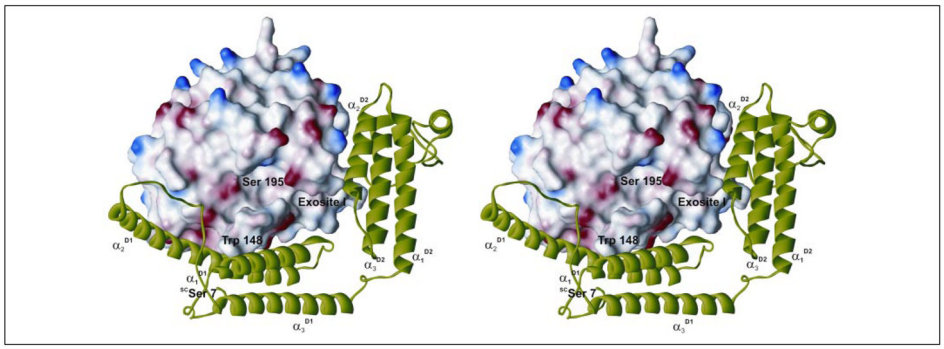

FIGURE 3. Crystal structure of the SC-(1–325)·bovine *α*-thrombin complex

The thrombin moiety is shown as a *solid surface* colored according to the electrostatic surface potential, from strongly negative (*deep red*) to strongly positive (*deep blue*). The boomerang-shaped SC molecule is comprised of the N-terminal domain D1 (helices α_1^{D1} to α_3^{D1}) and the C-terminal domain D2 (helices α_1^{D2} to α_6^{D2}) and is represented as a *green ribbon.* The anion-binding exosite I, the active site (Ser^{195}), and the 148 loop (Trp^{148}) of bovine *α*-thrombin are labeled. The N terminus of SC (defined from $^{SC}Ser^{7}$ onwards) is placed close to the Ile^{16} activation pocket of thrombin but is disordered in the complexes with bovine and human thrombin and extends away from the enzyme surface.

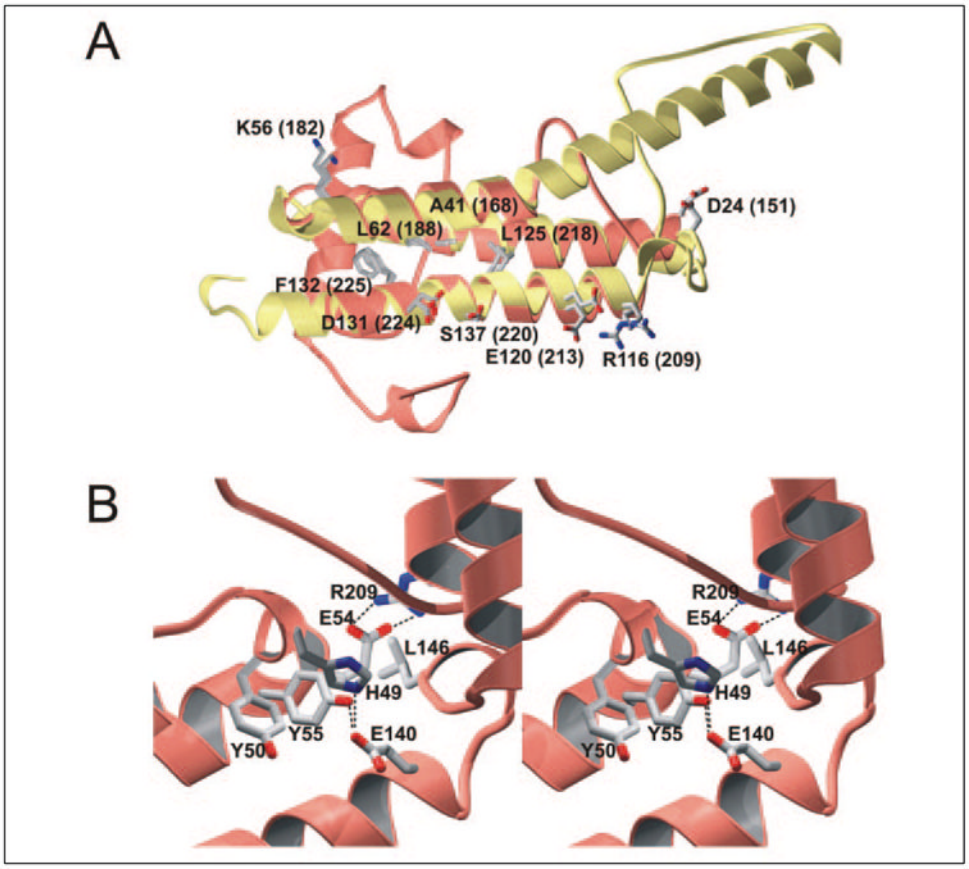

FIGURE 4. Structural characterization of SC-(1–325)

A, the two major helix bundles α_1^{D1}- α_3^{D1} (*yellow*) and α_1^{D2}-α_3^{D2} (*orange*), which are shown superimposed here, are structurally related. Side chains of all topologically equivalent residues conserved in both domains are shown with all their non-hydrogen atoms and labeled. *B*, close-up of the D1-D2 interdomain interface, with important residues shown with their full side chains. Notice the multiple contacts between polar/charged side chains (*e.g.* $^{SC}Glu^{54}$-$^{SC}Arg^{209}$), which separate the strictly conserved $^{SC}Leu^{146}$ side chain from bulk solvent.

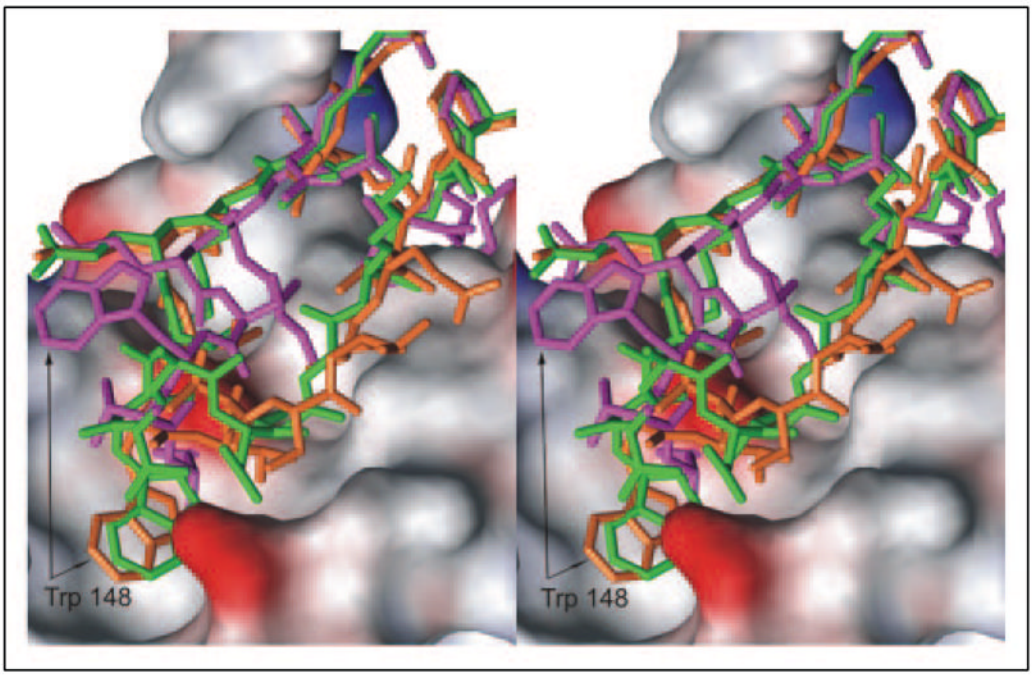

FIGURE 5. Staphylocoagulase binds to and stabilizes the 148 loop of (pre)thrombin

Stereo plot showing the superimposed 148 loops (residues Trp^{141}-Pro^{152}) of free, FPR-inhibited human thrombin (Protein Data Base code 1PPB) (27) (*purple*), SC-(1–325)-bound human Pre 2 (*green*), and SC-(1–325)-bound bovine thrombin (*orange*). The three loops are shown against the solid SC surface as seen in SC·human Pre 2, which is colored according to its electrostatic surface potential (*red*, negative; *blue*, positive). Notice in particular the insertion of the Trp^{148} indole ring in the SC groove lined by hydrophobic residues of helices α_1^{D1} and α_2^{D1} and the displacements of the following Thr^{149}-Gln^{151} segments in SC-(1–325) complexes with human Pre 2 and bovine thrombin compared with free human FPR-thrombin (partially hidden behind the SC surface). The small surface tube extending toward the top represents the inserted N-terminal SC segment.

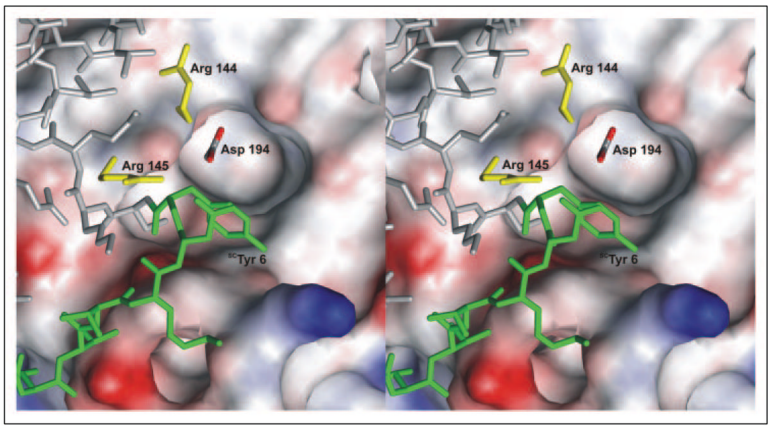

FIGURE 6. The SC N terminus would collide with Arg^{144}/Arg^{145} of bovine prethrombin

The *solid surface*, colored according to the electrostatic surface potential, shows the molecular surface of human Pre 2 around the Ile^{16} pocket, with the distal carboxylate group of Asp^{194} at its bottom. Notice the location of bovine thrombin-specific Arg^{144} and Arg^{145} (*yellow*). The stick model in front represents the N-terminal segment of SC (*green*, disordered residues ^{SC}Ile^{1} to ^{SC}Tyr^{6}) in complex with bovine thrombin. To insert its N-terminal residues into the Ile^{16} pocket of a bound bovine Pre 2 molecule, the cofactor main chain would have to change its direction at ^{SC}Lys^{8} to circumvent the Arg^{145} side chain. Because of collisions of the SC N terminus with the Arg^{144} and Arg^{145} side chains, its activator capability toward the bovine zymo-gen would be impaired or at least considerably weakened, as observed.

TABLE 1

Effect of SC-(1–325) binding to bovine ProT and α -thrombin on the hydrolysis of H-D-Phe-Pip-Arg-*p*NA

Michaelis-Menten kinetic parameters determined for hydrolysis of H-D-Phe-Pip-Arg-*p*NA by the indicated enzyme species are listed. The parameters were obtained by nonlinear least squares fitting of the Michaelis-Menten equation to the initial rates for the SC-(1–325)·bovine ProT complex or fitting of the integrated equation to progress curves for bovine α -thrombin in the presence and absence of saturating concentrations of SC-(1–325). The experiments were performed, and the data were analyzed as described under "Experimental Procedures."

Enzyme	k_{cat}	K_m	k_{cat}/K_m	K_i
	s^{-1}	μM	$\mu M^{-1} s^{-1} \times 10^{-3}$	μM
α-Thrombin	94 ± 2	3 ± 1	34,700	32 ± 2
SC-(1–325)3ProT	1.4 ± 0.1	140 ± 50	10	
SC-(1–325)3α-thrombin	68 ± 1	9 ± 1	7,400	39 ± 4

TABLE 2

Effect of SC-(1–325) binding on Fbg clotting activity of human and bovine (pro)thrombin

Fbg clotting activities were determined relative to human α -thrombin for the indicated enzyme species. The experiments were performed, and the data were analyzed as described under "Experimental Procedures." ND represents not detectable.

Species	Enzyme	Bovine Fbg	Human Fbg
		%	%
Human	α-Thrombin	25	100
	SC-(1–325)3ProT	25	70
	SC-(1–325)33-thrombin	30	111
Bovine	α-Thrombin	31	67
	SC-(1–325)3ProT	ND	0.07
	SC-(1–325)3α-thrombin	30	96

TABLE 3

Data collection and refinement statistics for the SC-(1–325)·bovine thrombin complex

Data collection	
Space group	C2
Cell constants	
a	183.78 Å
b	102.54 Å
c	134.04 Å
β	129.14°
Limiting resolution	3.50 Å
Reflections measured	138,556
Unique reflections	21,210
Completeness: overall, outermost shell (3.72–3.50 Å)	86.7%, 36.2%
Refinement	
Reflections used for refinement	21,210
Reflections in test set	420
Resolution range	31.7–3.50 Å
Completeness: overall, outermost shell (3.72–3.50 Å)	86.7%, 36.2%
R value, overall, outermost shell (3.72–3.50 Å)	0.233, 0.306
R_{free}, overall, outermost shell (3.72–3.50 Å)	0.266, 0.394
Root mean square deviations	
Bond lengths	0.008 Å
Bond angles	1.40°
Dihedral angles	21.3°
Improper angles	0.78°
Average *B* value	63.1 $Å^2$
Ramachandran plot	
Most favored region	75.2%
Additionally allowed region	22.7%
Non-hydrogen protein atoms	9,560
Non-hydrogen carbohydrate atoms	14
Non-hydrogen inhibitor atoms	60
Ions	2